

Supplemental information

This file includes:

Supplementary figures 1 to 4

Supplementary table 1 to 3

High-resolution structure of TBP with TAF1 reveals anchoring patterns in transcriptional regulation

Madhanagopal Anandapadamanaban¹, Cecilia Andresen^{1,6}, Sara Helander^{1,6}, Yoshifumi Ohyama², Marina I. Siponen^{3,5}, Patrik Lundström¹, Tetsuro Kokubo², Mitsuhiko Ikura⁴, Martin Moche³, and Maria Sunnerhagen^{1*}

¹Department of Physics, Chemistry and Biology (IFM), Linköping University, Linköping, Sweden.

²Division of Molecular and Cellular Biology, Graduate School of Nanobioscience, Yokohama City University, Yokohama, Japan.

³Department of Medical Biochemistry and Biophysics, Protein Science Facility, Karolinska Institutet, Stockholm, Sweden.

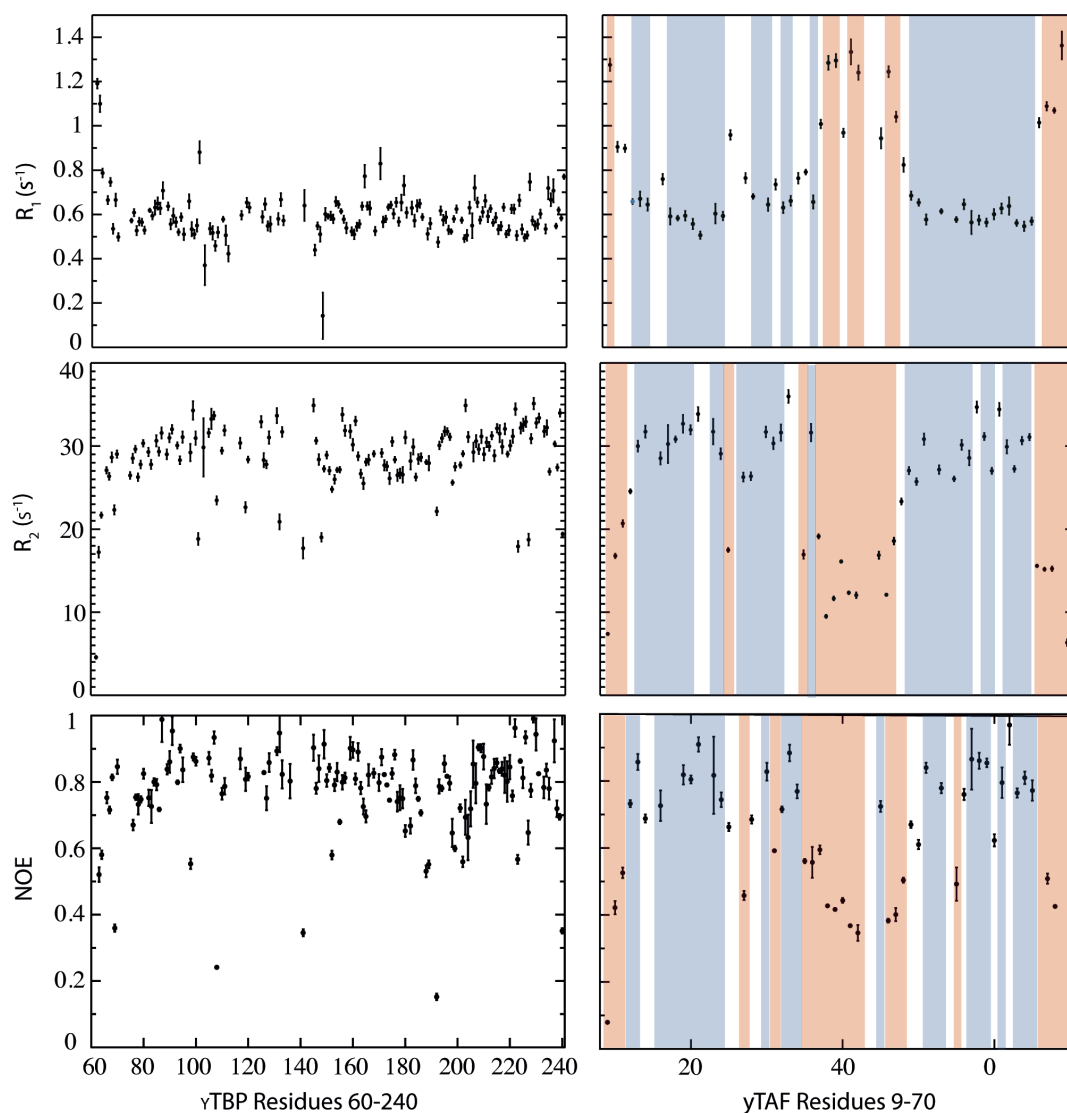
⁴Ontario Cancer Institute and Department of Medical Biophysics, University of Toronto, Toronto, Ontario, Canada.

⁵Current affiliation: Laboratoire de Bioénergétique Cellulaire, Saint-Paul-lez-Durance Cedex, France.

⁶ These authors contributed equally to this work.

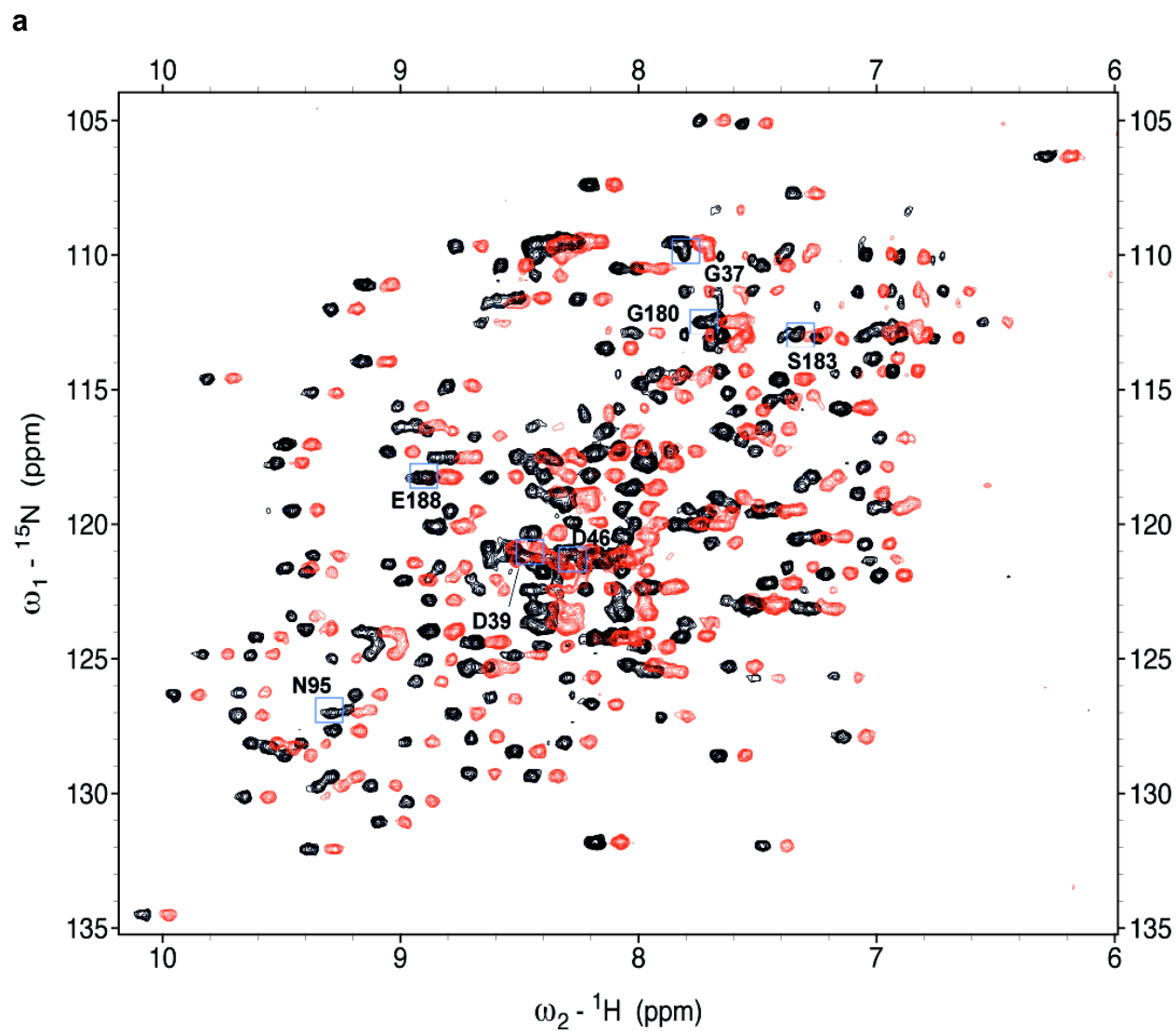
*Correspondence: maria.sunnerhagen@liu.se

Supplementary figure 1, Anandapadamanaban et al.



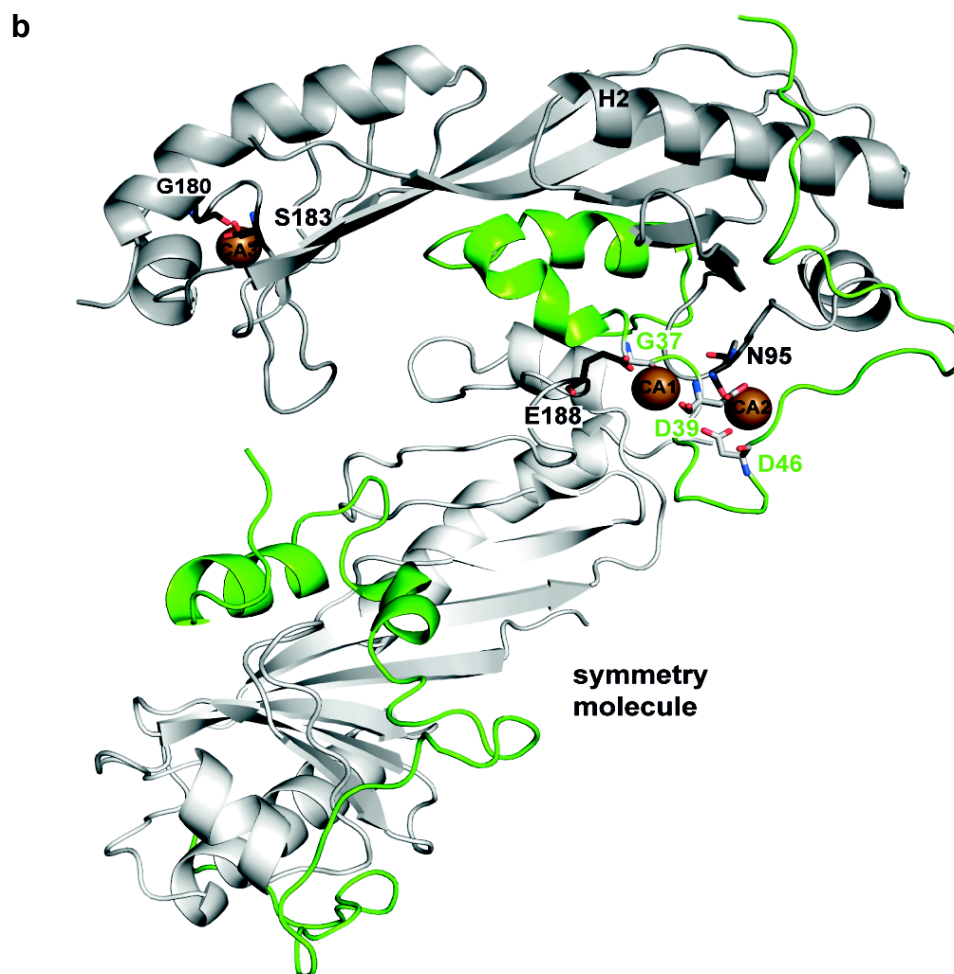
Supplementary figure 1, NMR ^{15}N -relaxation experiments of the yTAF1-yTBP fusion protein.

Relaxation data (R_1 , R_2 and NOE) for yTBP (left panel) and yTAF1 (right panel). Similar decay rates are obtained for a majority of the yTBP residues and for yTAF1 regions directly interacting with yTBP, suggesting a jointly folded protein complex. Marked in blue are the amino acids in yTAF that have decay rates that fall within the yTBP mean $\pm 2\sigma$ (R_1 ; 0.48-0.68, R_2 ; 25.47-33.68, NOE; 0.92-0.71). Residues in yTAF1 with decay rates exceeding $\pm 4\sigma$ from the yTBP mean are marked in red ($R_1 > 1.05$, $R_2 < 21.26$, NOE < 0.60), and are mainly located in the linker between the yTAND1 and yTAND2 regions or in the N- and C- termini. The ratio R_2/R_1 was used for calculations of the rotational correlation time of yTBP-yTAF1. The relaxation data were compatible with an axially symmetric rotational diffusion tensor, $D_{\perp} = D_{xx} = D_{yy}$, $D_{\parallel} = D_{zz}$, $\tau_{1,2,3} = (6D_{\perp})^{-1}, (5D_{\perp} + D_{\parallel})^{-1}, (2D_{\perp} + 4D_{\parallel})^{-1}$. The correlation times, $\tau_{1,2,3}$ were calculated to 17.1, 18.8 and 26.6 ns, respectively, in agreement with a monomeric yTBP-yTAF1 fusion protein in solution.



Supplementary figure 2a, NMR spectra of yTAF1-yTBP in the absence and presence of EDTA.

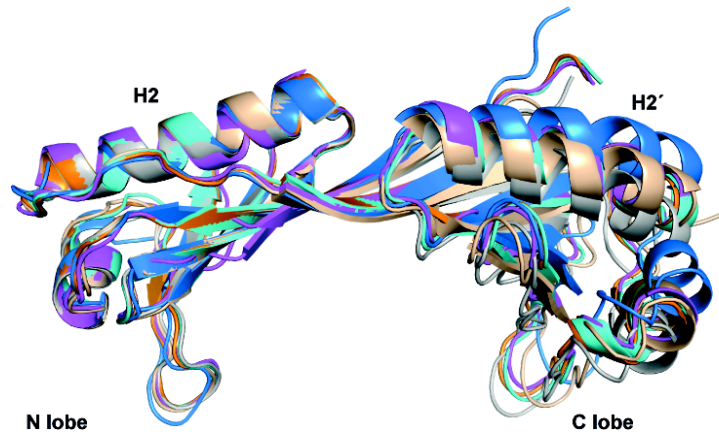
${}^{15}\text{N}$ TROSY spectra of yTAF1-yTBP in the absence (black) and presence (red) of 40 molar equivalents of EDTA to remove any residual Ca^{2+} ions. The red spectrum is shifted for clarity. The residues coordinating the tentative Ca^{2+} ions in the crystal structure are labelled and highlighted in the spectra.



Supplementary figure 2b, Tentative Ca^{2+} ions in the yTAF1-yTBP crystal structure. Sidechains coordinating the tentative Ca^{2+} ion are shown in sticks (yTBP-black and yTAF-green). The three Ca^{2+} ions are annotated as CA1, CA2 and CA3 (sand spheres).

The yTAND1-TAND2 linker region first protrudes out from the yTBP core domain in a loop-like structure, which is then again anchored towards yTBP-Y94 by TAND2 residues H50 and T48. Three ions with coordination schemes suggesting Ca^{2+} are found in this region (b), however their B-factors are fairly high. NMR experiments in the presence and absence of excess Ca^{2+} or EDTA did not reveal any chemical shift differences (a), showing that these ions are not tightly bound in solution. This region is also involved in crystal contacts (b), which may account for the presence of the ions in the crystal.

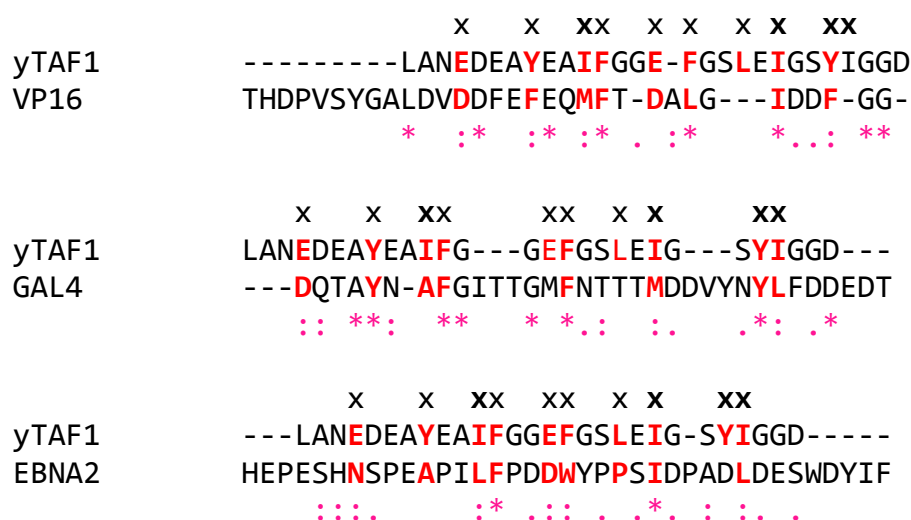
Supplementary figure 3, Anandapadamanaban et al.



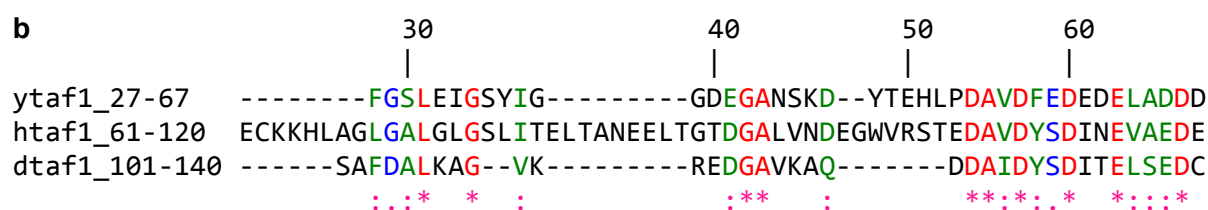
Supplementary figure 3, Relative orientation of N lobe and C lobe in yTBP structure. The yeast TBP structures were superimposed using only main chain atoms of the H2 helix. The yeast TBPs of yTBP-yTAF1 (grey), TBP-DNA (1YTB, cyan), TBP-Brf1 (1NGM, magenta), TBP-TFI-IA-DNA (1NH2, orange) and TBP dimer (1YTB, chain A-marine blue and chain B –wheat) are shown in cartoon representation with the annotated secondary structures.

Supplementary figure 4, Anandapadamanaban et al.

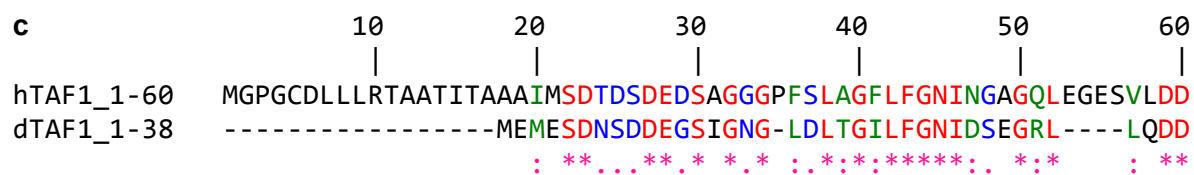
a



b



c



Supplementary figure 4, ClustalW alignments of TAD domains. a) Alignment of transcriptional activators yTAF1₁₂₋₃₉, EBNA2₄₂₆₋₄₆₂, GAL4₈₄₂₋₈₇₄ and VP16₄₅₇₋₄₉₀. TAF1 residues labeled ‘x’ and red interact with TBP in the current structure; boldfaced ‘x’ contact TBP-L114 in the concave, DNA-binding surface, where a mutation to K disrupts binding with yTAF1, EBNA2, GAL4 and VP16¹⁸. Conservation with transcriptional activation domains from VP16, Gal4 and EBNA2 in TBP-contacting residues is indicated in bold/red. Sequence similarity indicated according to ClustalW conventions. b) Alignment of hTAF1 with yTAF1 and dTAF1 shows joint sequence similarities in the yTAF1-TAND2 region (residues 53-67)²⁹ and in the second helix of yTAF1-TAND1 (residues 27-37), which respectively bind the TBP convex surface groove and DNA-binding TBP concave surface (Figure 1, Anandapadamanaban et al). Numbering according to yTAF1. c) The N-terminal part of hTAF1 shows sequence similarity with dTAF1 residues 11-38, which bind the TBP DNA-binding groove in a manner distinct from the binding of yTAF1 residues 27-37 to the same TBP surface (Figure 5c, Anandapadamanaban et al.). Numbering according to hTAF1. Together with b), this suggests that while yTAF1 contains a single motif binding the TBP DNA-binding groove, hTAF1 and dTAF1 contain multiple sequence segments capable of interacting with the same TBP surface, in addition to the jointly conserved and functionally equivalent TAND2 motif²⁹ binding the TBP convex surface.

Supplementary table 1, Anandapadamanaban et al.

Interacting residues and hydrogen bond distance in the yTBP-yTAF1 interface.

yTBP atom	-----	yTAF1 atom	Distance (Å)
A86 [O]	-----	H50 [ND1]	2.67
L87 [O]	-----	L51 [N]	2.87
H88 [O]	-----	V55 [N]	3.73
R90 [O]	-----	H50 [NE2]	3.62
R90 [N]	-----	V55 [O]	2.97
N91 [OD1]	-----	F57 [N]	3.07
E93 [OE1]	-----	D39 [N]	2.98
Y94 [O]	-----	T48 [OG1]	3.72
Y94 [N]	-----	T48 [OG1]	3.02
R98 [NH1]	-----	G38 [O]	3.18
A100 [N]	-----	L12 [O]	2.89
R105 [NH2]	-----	I36 [O]	2.77
R105 [NH2]	-----	G37 [O]	3.47
R107 [N]	-----	E58 [O]	2.85
A117 [N]	-----	E15 [OE2]	3.55
S118 [N]	-----	E15 [OE2]	2.93
K133 [NZ]	-----	D66 [OD2]	2.98
R137 [NE]	-----	A64 [O]	2.92
R137 [NH2]	-----	A64 [O]	3.09
R137 [O]	-----	A64 [N]	2.96
K138 [NZ]	-----	E60 [O]	3.00
R141 [NE]	-----	E62 [OE1]	3.13
R141 [NH2]	-----	E62 [OE1]	3.16
K145 [NZ]	-----	E60 [OE1]	2.96
K145 [NZ]	-----	E60 [OE2]	3.03

Supplementary table 1, Interacting residues and hydrogen bond distance in the yTBP-yTAF1 interface. PDBePISA (Protein Interfaces, Surfaces and Assemblies) was used to identify the hydrogen bonds and calculate the distance.

Supplementary table 2, Anandapadamanaban et al.

S. cerevisiae strains used in this study

Strain*	Genotype
YTK11411	<i>MATa his3Δ1 leu2Δ0 ura3Δ0 met15Δ0 Δtaf1::kanMX6 pYN1/TAF1</i>
YTK12029	<i>MATa his3Δ1 leu2Δ0 ura3Δ0 met15Δ0 Δtaf1::kanMX6 pM4770/TAF1</i>
YTK12083	<i>MATa his3Δ1 leu2Δ0 ura3Δ0 met15Δ0 Δtaf1::kanMX6 pM7121/taf1-ΔTAND</i>
YTK13412	<i>MATa his3Δ1 leu2Δ0 ura3Δ0 met15Δ0 Δtaf1::kanMX6 pM7280/taf1-E60A E62A</i>
YTK13413	<i>MATa his3Δ1 leu2Δ0 ura3Δ0 met15Δ0 Δtaf1::kanMX6 pM7281/taf1-E60A E62A D66A</i>
YTK13414	<i>MATa his3Δ1 leu2Δ0 ura3Δ0 met15Δ0 Δtaf1::kanMX6 pM7282/taf1-E58A D59A</i>
YTK13415	<i>MATa his3Δ1 leu2Δ0 ura3Δ0 met15Δ0 Δtaf1::kanMX6 pM7283/taf1-E58A D59A E60A E62A</i>
YTK13416	<i>MATa his3Δ1 leu2Δ0 ura3Δ0 met15Δ0 Δtaf1::kanMX6 pM7284/taf1-H50A</i>
YTK13417	<i>MATa his3Δ1 leu2Δ0 ura3Δ0 met15Δ0 Δtaf1::kanMX6 pM7285/taf1-H50G</i>
YTK13428	<i>MATa his3Δ1 leu2Δ0 ura3Δ0 met15Δ0 Δtaf1::kanMX6 pM7118/TAF1</i>
YTK13429	<i>MATa his3Δ1 leu2Δ0 ura3Δ0 met15Δ0 Δtaf1::kanMX6 pM7119/taf1-ΔTAND</i>
YTK13430	<i>MATa his3Δ1 leu2Δ0 ura3Δ0 met15Δ0 Δtaf1::kanMX6 pM7286/taf1-ΔTAND1</i>
YTK13431	<i>MATa his3Δ1 leu2Δ0 ura3Δ0 met15Δ0 Δtaf1::kanMX6 pM7287/taf1-ΔTAND1 E60A E62A</i>
YTK13432	<i>MATa his3Δ1 leu2Δ0 ura3Δ0 met15Δ0 Δtaf1::kanMX6 pM7288/taf1-ΔTAND1 E60A E62A D66A</i>
YTK13433	<i>MATa his3Δ1 leu2Δ0 ura3Δ0 met15Δ0 Δtaf1::kanMX6 pM7289/taf1-ΔTAND1 E58A D59A</i>
YTK13434	<i>MATa his3Δ1 leu2Δ0 ura3Δ0 met15Δ0 Δtaf1::kanMX6 pM7290/taf1-ΔTAND1 E58A D59A E60A E62A</i>
YTK13435	<i>MATa his3Δ1 leu2Δ0 ura3Δ0 met15Δ0 Δtaf1::kanMX6 pM7291/taf1-ΔTAND1 H50A</i>
YTK13436	<i>MATa his3Δ1 leu2Δ0 ura3Δ0 met15Δ0 Δtaf1::kanMX6 pM7292/taf1-ΔTAND1 H50G</i>
YTK13444	<i>MATa his3Δ1 leu2Δ0 ura3Δ0 met15Δ0 Δtaf1::kanMX6 pM7298/taf1-ΔTAND2</i>
YTK13536	<i>MATa his3Δ1 leu2Δ0 ura3Δ0 met15Δ0 Δtaf1::kanMX6 pM7320/taf1-ΔTAND1 F57A</i>

* YTK 11411 12029 were first constructed in Ohshima et al., 2010. All other strains were constructed for this study.

Supplementary table 2, *S. cerevisiae* strains used in this study.

Supplementary table 3, Anandapadamanaban et al.

Oligonucleotides used in this study

Number	Sequence
T869	5'-ACACACGAATTCTTATGGCAAATCGTCATCGTCATC-3'
T903	5'-AAGCAGCAGGGATCCGGCAAGTCTGATGCTAATTTGCATCCA-3'
TK43	5'-TAAAGCAGCAGGGATCCGCGCAATTCAAAGGACTATAC-3'
TK48	5'-TGCCGGATGCTGTAGATGCTGAAGATGAAGATGAAC-3'
TK125	5'-GTGTCCTCCTCTAACAAT-3'
TK344	5'-CACGGATCCGGCAAGACCAAC-3'
TK12085	5'-CTGTAGATTTTGAAGATGCAGATGCACTTGCTGATGACGATG-3'
TK12086	5'-GTAGATTTTGAAGATGCAGATGCACTTGCTGATGCAGATGACGATTTGCC-3'
TK12087	5'-CGGATGCTGTAGATTTTGCAGCTGAAGATGAAGTGGCTGAT-3'
TK12088	5'-CGGATGCTGTAGATTTTGCAGCTGCAGATGCACTTGCTGATGACGATG-3'
TK12089	5'-CAAAGGACTATACGGAGGCTTTGCCGGATGCTGTAG-3'
TK12090	5'-CAAAGGACTATACGGAGGCTTTGCCGGATGCTGTAG-3'

Supplementary table 3, Oligonucleotides used in this study.